Calculated acoustic plasmon spectra in GaSb, SnTe and Bi

1989 J. Phys.: Condens. Matter 1 8877

(http://iopscience.iop.org/0953-8984/1/45/013)

J. Phys.: Condens. Matter 1 (1989) 8877–8886. Printed in the UK

Calculated acoustic plasmon spectra in GaSb, SnTe and Bi

B Bennacer, A A Cottey and J Senkiw
School of Physics, University of East Anglia, Norwich NR4 7TJ, UK

Received 13 February 1989, in final form 23 May 1989

Abstract. We present RPA calculations of the spectra of acoustic plasmons in GaSb, SnTe and Bi. We find that acoustic plasmons only just exist in Bi, having a small critical wavevector of about 10 μm^{-1}, beyond which they do not exist. In n-GaSb with 1.4×10^{24} electrons/m^3, the calculations give an acoustic plasmon with velocity about 10^5 m s^{-1} and relative damping $|\omega''|/\omega'$ about 0.1. The acoustic plasmon exists for wavevectors up to at least 100 μm^{-1} (where the RPA breaks down). In p-SnTe with 1.5×10^{26} holes/m^3, we find an acoustic plasmon with velocity about 2×10^5 m s^{-1} and relative damping about 0.1. The spectrum ends abruptly at a critical wavevector which is about 100 μm^{-1}. We conclude that the prospects for observing acoustic plasmons are poor in Bi, but good in GaSb and SnTe.

1. Introduction

An acoustic plasmon is a longitudinal oscillation of the carriers of a two-component plasma, with the polarisations of the two components out of phase and partially cancelling. Acoustic plasmons in a two-component degenerate Fermi system were first studied by Silin (1952). Since then there has been a trickle of theoretical papers and little published experimental work on these excitations. The introductory section of Bennacer and Cottey 1989 (BC) outlines briefly the historical development. There is still no definite experimental proof that acoustic plasmons exist in a homogeneous two-component degenerate Fermi system.

Interest in acoustic plasmons has however recently revived, because of their possible role in high-T_c superconductivity. Little (1988) has reviewed the known experimental constraints on theories of high-T_c superconductivity. He concludes that a successful theory should have virtually all the attributes of the BCS theory. The one important difference is that charge carrier pairing should be mediated, not by phonons, but by some charged excitation with an energy several times that of phonons. Theories of high-T_c superconductivity involving acoustic plasmons have been proposed by Ruvalds (1987) and Griffin (1988). Canright and Vignale (1988) report, however, in a pre-publication abstract that acoustic plasmons contribute little to superconductivity in their model of a two-dimensional two-component electron gas. (Other models involving plasmons, but not acoustic plasmons, include the soft-plasmon model of Ashkenazi *et al* (1987), and the collective polarisation wave model of Vigneron *et al* (1988).

0953-8984/89/458877 + 10 $02.50

Our purpose in the present paper is to apply the general theoretical analysis of BC to simple materials. We think that the possible relevance of acoustic plasmons to high-T_c superconductors renders timely the further development of theory and experiment in simple materials. Strengthening the foundations would permit more reliable application to complex materials.

BC gives a general survey of the acoustic plasmon spectra for practicable semimetal and degenerate semiconductor parameters, and an application of the theory to the GaAs electron–hole plasma (for which experimental spectroscopy was done by Pinczuk *et al* 1981). In the present paper we give the results of calculations of the acoustic plasmon spectrum for GaSb, SnTe and Bi.

2. The two-component plasma model

We model the charge carriers in semimetals and semiconductors as a two-component degenerate fermi gas. The two components are labelled by $i(=1,2)$, and component i has ν_i spherical pockets, all equivalent by symmetry, with Fermi wavevector k_{F_i}, Fermi velocity v_{F_i}, Fermi energy e_{F_i}, effective mass m_i^* and $e_{F_i} = \hbar^2 k_{F_i}^2/2m_i^*$. We label the two plasmas such that $v_{F_2} \leqslant v_{F_1}$.

We treat the ions in a jellium model, which supplies a constant background relative permittivity ε_{bg}. The value of ε_{bg} can be large so the high-density limit $(r_s^* \leqslant 1)$ can be reached. This is indeed the case in the systems studied here.

We consider a plasma wave $\sim \exp \mathrm{i}(qx - \omega t)$ with q real and positive, with complex frequency $\omega = \omega' + \mathrm{i}\omega''$ $(\omega' > 0)$. We define the dielectric function $\varepsilon(q, \omega)$ as (permittivity of system)$/\varepsilon_0\varepsilon_{bg}$, where ε_0 is the permittivity of the vacuum. The dielectric function ε of the two-component plasma, allowing only intra-pocket transitions, is given by

$$\varepsilon(q, \omega) = 1 - (e^2/\varepsilon_0\varepsilon_{bg}q^2)(\chi_1 + \chi_2)$$

where χ_i $(i = 1, 2)$ is the polarisation function of the component i.

We use the random phase approximation (RPA) with exact analytic continuation to the lower half of the complex frequency plane (Cottey 1985, BC) to get an explicit form for ε. We find it convenient to introduce the reduced plasmon velocity and wavevector

$$u = \omega/qv_{F_2} \qquad z = q/2k_{F_2}.$$

We also write r_v for v_{F_2}/v_{F_1} and r_k for k_{F_2}/k_{F_1}. Then ε is given (BC) by

$$\varepsilon(z, u) = 1 + 2c_1\nu_1 g(r_k z, r_v u) + 2c_2\nu_2 g(z, u)$$

where

$$g(z, u) = (2z)^{-2}\{\tfrac{1}{2} + (8z)^{-1}[\mathcal{F}(z-u) - \mathcal{F}(-z-u)]\}$$

$$\mathcal{F}(\zeta) = (1-\zeta^2)\{\ln[(\zeta+1)/(\zeta-1)]\} + \Delta\mathcal{F}$$

$$\Delta\mathcal{F}(\zeta) = \begin{cases} 2\pi i(1-\zeta^2) & (\zeta'^2 < 1 + \zeta''^2 \text{ and } \zeta'' > 0) \\ 0 & (\text{otherwise}) \end{cases}$$

$$\zeta = \zeta' + i\zeta''$$

and

$$c_i = (2/\pi)(4/9\pi)^{1/3} r^*_{sspi} \approx (1/3) r^*_{sspi} \qquad (i = 1, 2)$$

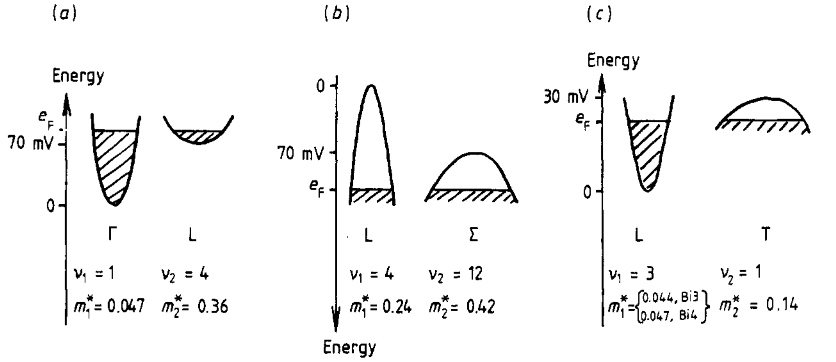

Figure 1. The band models of the materials studied (*a*), GaSb (zincblende structure); (*b*), SnTe (rocksalt structure); (*c*) Bi (rhombohedral).

are convenient density parameters. $r^*_{\text{ssp}i}$ is the standard reduced density parameter for a single pocket (sp) of component i, defined by

$$(4\pi/3)(r^*_{\text{ssp}i}a^*_{\text{B}i})^3 = \nu_i/n_i$$

where n_i is the carrier density of component i with all pockets counted and $a^*_{\text{B}i}$ is the reduced Bohr radius for component i, i.e. $4\pi\varepsilon_0\varepsilon_{\text{bg}}\hbar^2/e^2m_i^*$.

The function $\varepsilon'(\varepsilon = \varepsilon' + \text{i}\varepsilon'')$ is discontinuous on the lines

$$u' = |(1 + u''^2)^{1/2} \pm z| \qquad \text{and} \qquad u' = |(r_v^{-2} + u''^2)^{1/2} \pm (r_k z)/r_v|$$

but ε'' is continuous. The discontinuities are consequences of the discontinuity of the Fermi–Dirac function at zero temperature.

The dispersion relations for plasmons are the solutions of $\varepsilon(q, \omega) = 0$. In a two-component system there is always an 'ordinary plasmon' branch (with $\omega \to \omega_\text{P}$ as $q \to 0$). The acoustic plasmon branch (with $\omega/q \to$ constant as $q \to 0$) exists for a range of wavevectors q from zero to some sharp cut-off q_c, for some values of the system parameters $c_2\nu_2$, $c_1\nu_1$, r_v and r_k. The range of values of these parameters in which acoustic plasmons exist is discussed in BC.

In the results of BC an acoustic plasmon is invariably subject to Landau damping by plasma 1 but not by plasma 2. Now the maximum energy of a particle–hole pair in plasma 2 is $\hbar^2q(q + 2k_{\text{F}_2})/2m_2^*$, which would be the line $z + 1$ in the u–z figures 2–7. With allowance for finite damping (BC), the onset of Landau damping by plasma 2 is when the real part of u, u', meets the curve $z + (1 + u''^2)^{1/2}$. This curve is plotted in each of figures 2–7. When u' meets this curve (at a critical wavevector $q_c = 2k_{\text{F}_2}z_c$) the acoustic plasmon abruptly ceases to exist. The spectra of SnTe and Bi, figures 4–7, have such a cut-off, and it is less than the maximum wavevector ($q_{\text{max}} = 2k_{\text{F}_2}z_{\text{max}}$) for which the RPA is valid. In GaSb on the other hand, $z_{\text{max}} < z_c$, and the results are given for $0 \leqslant z \leqslant z_{\text{max}}$ (figures 2, 3).

3. Results

3.1. GaSb

We assume a simple 'metallic' model (Fistul' 1969) of strongly n-doped GaSb, with electrons occupying four subsidiary L minima as well as the Γ minimum (figure 1(*a*)).

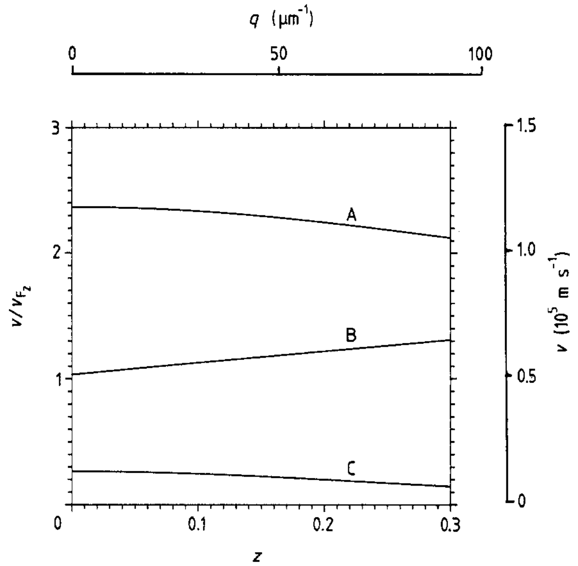

Figure 2. Real and imaginary parts of the acoustic plasmon velocity versus wavevector for GaSb system G1, with carrier density $n = 1.4 \times 10^{24}$ m^{-3} and Fermi energy $e_F = 72.5$ meV. The graph ends around the wavevector at which the RPA breaks down. A, Re (acoustic plasmon velocity); B, upper edge of particle–hole pair continuum of plasma 2; C, |Im (acoustic plasmon velocity)|.

The necessary high carrier concentration can be achieved (Kauschke *et al* 1987). The values of m_1^* and m_2^* are from Hilsum and Rose-Innes (1961, p 56) and Hilsum (1966) respectively. The two systems studied are Gl with $n = 1.4 \times 10^{24}$ carriers/m^3, $e_F = 72.5$ meV and G2 with $n = 2.3 \times 10^{24}$ carriers/m^3, $e_F = 75$ meV.

The acoustic plasmon energies which we calculate always turn out to be well below that of the transverse optic phonon at zero wavevector in GaSb, which is 28 meV (Farr *et al* 1975). Therefore the appropriate value of ε_{bg} is $\varepsilon_{bg_0} = 15$ (Hilsum and Rose-Innes 1961, p 181). The carrier density is sufficient (BC) for validity of the RPA, but the maximum wavevector at which the RPA is valid ($z_{max} = 0.3$) is less than the wavevector z_c at which the acoustic plasmon spectrum ends. The results u' and $|u''|$ against z are shown for $0 \leqslant z \leqslant 0.3$ in figures 2 and 3.

3.2. SnTe

SnTe is a p-type semimetal (figure 1(b)), the carrier concentration p depending on the conditions of production. For the values of p considered here, the crystal structure is extremely close to the rocksalt structure (Cottey *et al* 1987). Band structure calculations have been performed for this structure (Cohen and Tsang 1971, Melvin and Hendry 1979), and these results are invariably used in analysing the properties of SnTe. For the hole concentration considered here, there are 4 L pockets (plasma 1) and 12 Σ pockets (plasma 2). The values of m_1^* and m_2^* (figure 1(b)) which we use are best values around the Fermi energies of the systems we studied, based on the band structures of Cohen and Tsang (1971) and of Melvin and Hendry (1979).

The transverse optic phonon in SnTe is soft at small wavevector, with $\omega_{To} \simeq 2$ meV (Jantsch *et al* 1983, p 6), whereas we find the acoustic plasmons exist with frequencies

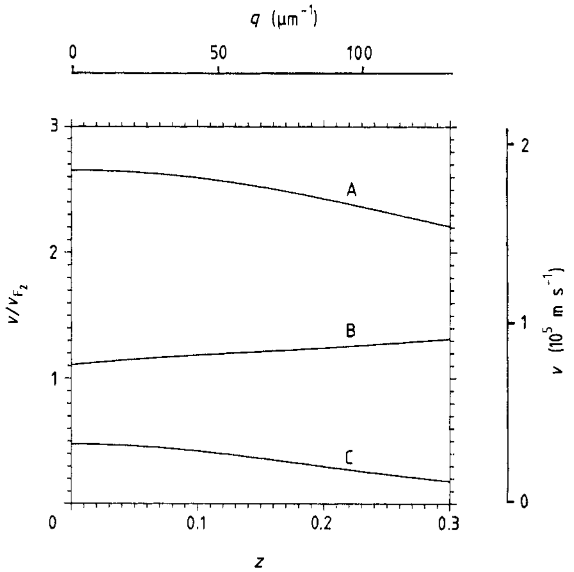

Figure 3. As for figure 2, but for GaSb system G2, with $n = 2.3 \times 10^{24}\ \mathrm{m^{-3}}$ and $e_F = 75$ meV.

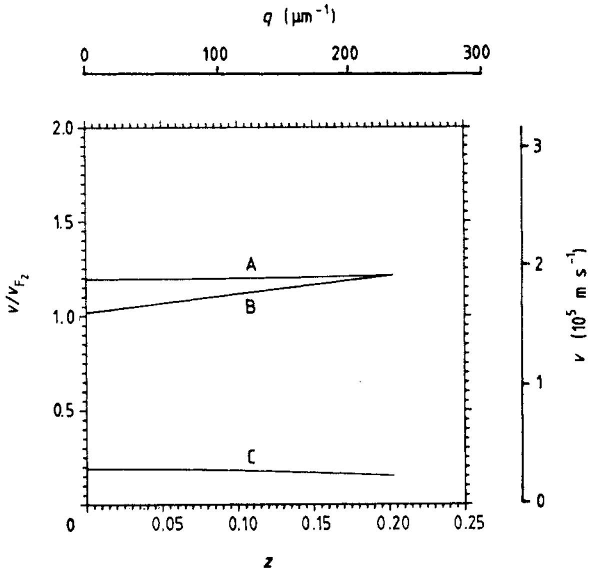

Figure 4. Spectrum for SnTe system S1, with hole concentration $p = 2.2 \times 10^{26}\ \mathrm{m^{-3}}$ and $e_F = 100$ meV. The spectrum ends abruptly at $z = 0.2$, when it meets the particle–hole continuum of the slower species (in the Σ pockets). Curve labelling is as in figure 2.

up to 29 meV for system S1 (figure 4) and up to 12 meV for system S2 (figure 5). Thus for most of the acoustic plasmon spectrum the frequency is well above ω_{To}, and the appropriate value of $\varepsilon_{\mathrm{bg}}$ is $\varepsilon_{\mathrm{bg}\infty} = 45$ (Reidl *et al* 1965). For sufficiently small wavevectors the acoustic plasmon frequency is less than ω_{To} and the appropriate value of $\varepsilon_{\mathrm{bg}}$ is $\varepsilon_{\mathrm{bg}0}$, which is very large (Jantsch *et al* 1983). It was shown however in BC that the complex

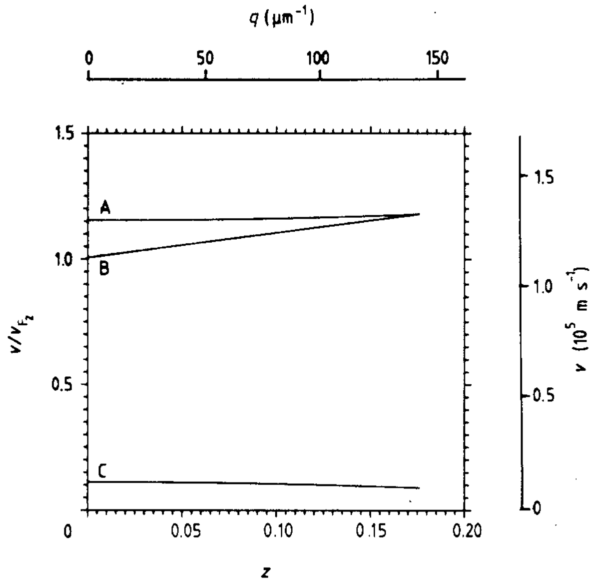

Figure 5. Spectrum for SnTe system S2, with $p = 1.5 \times 10^{26}\ \text{m}^{-3}$, $e_F = 85$ meV. Curve labelling is as in figure 2.

reduced velocity u is independent of reduced density (and hence of ε_{bg}) in the limit $q \rightarrow 0$. We have therefore neglected the interaction between the optic phonon and the acoustic plasmon. The resulting acoustic plasmon spectrum is correct except for energy near ω_{To}, where a typical 'mode-crossing' interaction may be anticipated.

The SnTe spectra meet the reduced Σ-particle–hole pair continuum at $z_c \simeq 0.2$, and this is well within the range of validity of the RPA ($z_{max} \simeq 0.4$ and 0.5 for systems S1 and S2 respectively).

3.3. *Bi*

The relevant band structure of Bi is shown in figure 1(*c*). The mass values are the best spherical values, calculated at the Fermi energies of the systems studied, using the ellipsoidal non-parabolic band model of Smith *et al* (1964). The effect of the ellipsoidal nature of the pockets is described in the Appendix.

By virtue of the small energy gap at L, the conditions for the Lyddane–Sachs–Teller relation do not hold for Bi, and ε_{bg} is independent of frequency in the range considered. We use a direction averaged value $\varepsilon_{bg} = 88$ from the data of Gerlach *et al* (1976).

System Bi3 is undoped Bi ($n_e = n_h$). The main feature of the acoustic plasmon spectrum (figure 6) is that it barely exists. It starts (i.e. at $q = 0$) close to the T particle–hole pair continuum and meets it at a small wavevector, $z_c \simeq 0.02$. That the acoustic plasmon barely exists can also be seen from the point of view of the $q = 0$ special case of the theory (Cottey 1985, BC). It is shown there that $u(0)$, i.e. u at $q = 0$, depends only on two parameters: the ratio of Fermi velocities of the two plasmas, $r_v = v_{F_2}/v_{F_1}$; and the ratio of Thomas–Fermi screening wavevectors, $R^{1/2} = \kappa_{TF_2}/\kappa_{TF_1}$. These parameters take, for system Bi3, the values $R = 1.54$, $r_v = 0.45$. These parameters are near to the edge of the existence domain in $R - r_v$ space (Cottey 1985, BC).

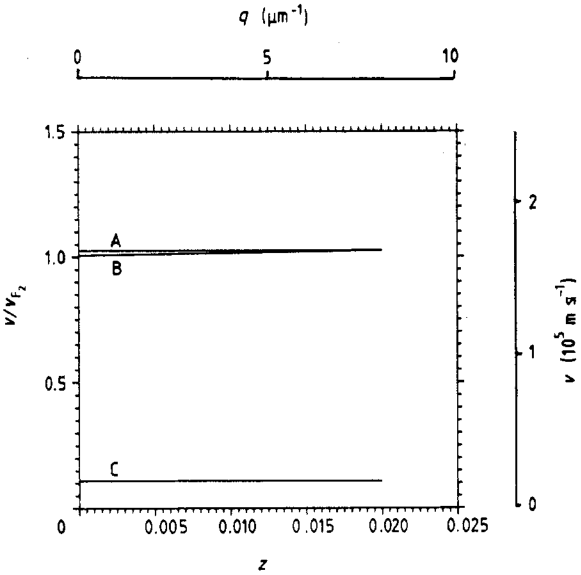

Figure 6. Spectrum for Bi system Bi3 (undoped Bi) with $n_e = n_h = 2.7 \times 10^{23}\,\mathrm{m}^{-3}$ and $e_F = 28\,\mathrm{meV}$. The critical wavevector is small; the acoustic plasmon only just exists. Curve labelling is as in figure 2.

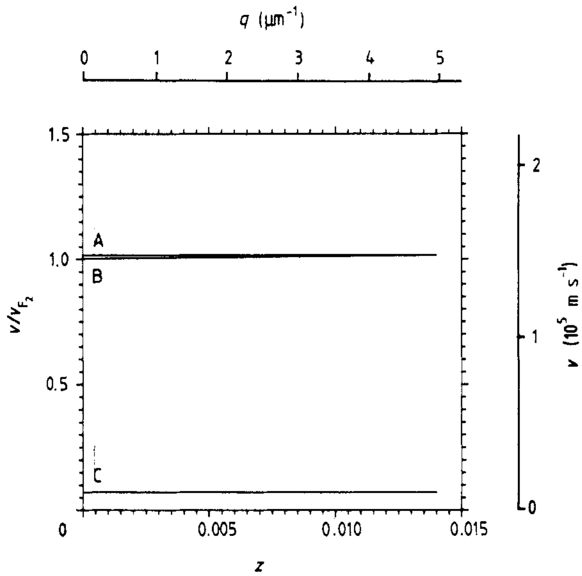

Figure 7. Spectrum for Bi system Bi4 (n-doped Bi) with $n_e = 3.4 \times 10^{23}\,\mathrm{m}^{-3}$, $n_h = 1.9 \times 10^{23}\,\mathrm{m}^{-3}$ and $e_F = 30\,\mathrm{meV}$. Curve labelling is as in figure 2.

On the basis of the surveyable $q = 0$ theory, we were also able to consider whether doping Bi, either n-type or p-type, would lead to parameters more favourable for acoustic plasmons. The answer is 'no'. Figure 7 shows the results for n-doped Bi with donor concentration $n_d = n_e - n_h = 1.5 \times 10^{23}\,\mathrm{m}^{-3}$.

4. Conclusion

Although acoustic plasmons have long been predicted, they have not been observed unambiguously in a homogeneous two-component degenerate Fermi plasma. Earlier discussions of acoustic plasmons have usually been based on the Pines–Froehlich approximation ($v_{F_2} \ll v \ll v_{F_1}$), and often also with the restrictions $\nu_2 = \nu_1$, $k_{F_2} = k_{F_1}$. In this case, the condition for weakly damped acoustic plasmons is $m_1 \ll m_2$. Partly on this basis, Bi has (sometimes implicitly, in that it has been much studied) been considered a good candidate for acoustic plasmons (McWhorter and May 1964, Olivei 1971, Ruvalds 1981).

Our analysis, which treats damping and finite wavevector exactly (within the RPA), shows that Bi is a poor candidate for acoustic plasmons. The principal weakness of the results of figures 6 and 7 is the neglect of the ellipsoidal nature of the pockets, which is very pronounced in Bi. We give in the Appendix the results for zero wavevector, allowing for ellipsoidal pockets. These results are based on the Pines–Froehlich approximation; the corrections must be regarded as only a rough guide. The ellipticity of the electron pockets (the faster component) does not enter the expression (A1.1) for the direction ($\hat{n}$) dependent velocity $v(\hat{n})$. The eccentricity of the hole pocket (the slower component), which is considerably less than that of the electron pockets, does influence $v(\hat{n})$. The onset of Landau damping by the holes varies with $\hat{n}$ in the same way as $v(\hat{n})$. The acoustic plasmon is expected to exist, but only for small wavevectors, in all directions $\hat{n}$.

Because of the cubic symmetry, v for GaSb and SnTe (allowing for ellipsoidal pockets) is independent of $\hat{n}$ at $q = 0$. Allowing for eccentricity of the Σ pockets in SnTe increases v, above the result of the spherical pocket model, by 25%. The magnitude of the critical wavevector in SnTe does depend on $\hat{n}$, when ellipticity is allowed for. We expect acoustic plasmons to propagate in the [100] and [110] directions, but not in the [111] direction.

We believe the prospects for observing acoustic plasmons in strongly doped n-GaSb, and in SnTe, are good, on the grounds: (i) that the relative damping is small ($|\omega''|/\omega' \sim 0.1$ in each case reported here); and (ii) that the modes exist up to reasonably large wavevectors ($\sim 100\ \mu m^{-1}$).

Acknowledgment

B Bennacer thanks the Algerian Ministry of Higher Education for a research grant.

Appendix A1: Notes on the generalisation to ellipsoidal pockets

In the case of spherical pockets which we considered so far in this paper and in BC, the ν_1 pockets of plasma 1 were equivalent to each other, and the ν_2 pockets of plasma 2 were equivalent to each other. If the pockets are now ellipsoidal, then for $q > 0$ and arbitrary direction $\hat{n}$ of the plasma wave, we need to identify the symmetry sets of pockets which are equivalent to each other and also have equivalent relationships to $\hat{n}$. The number I of such sets is in general greater than 2. Furthermore the normal modes are, in general, purely longitudinal only when $\hat{n}$ lies along certain symmetry directions. We are currently investigating the general problem. Here we mention some provisional expectations and results.

From our experience with solutions of two- and three-component plasmas with spherical pockets (BC) we anticipate (along a direction in which pure longitudinal modes exist), one ordinary plasmon and a number J of acoustic plasmons with $0 \leqslant J \leqslant I - 1$. We further expect J to be small (usually 0 or 1) for real systems.

In the Pines–Fröhlich approximation ($v_{F_2} \ll v \ll v_{F_1}$ and q small), the problem can be solved analytically for arbitrary $\hat{\boldsymbol{n}}$. The result is a single acoustic plasma mode with the direction-dependent speed $v(\hat{\boldsymbol{n}})$ given by

$$v(\hat{\boldsymbol{n}})/\bar{v} = \left[\sum_{\mu=1}^{\nu_2} \hat{\boldsymbol{n}} \boldsymbol{\alpha}_{2\mu} \hat{\boldsymbol{n}} / \bar{\alpha}_2 \nu_2 \right]^{1/2} \tag{A1.1}$$

Here $\boldsymbol{\alpha}_{2\mu}$ is the inverse mass tensor of pocket μ of component 2, $\bar{\alpha}_2$ is the equivalent spherical inverse mass ($= (\det \boldsymbol{\alpha})^{1/3}$), and $\bar{v}$ is the acoustic plasmon velocity in the equivalent spherical model. The correction depends on the eccentricity of the pockets of component 2 only.

For a cubic crystal the right side of equation (A1.1) becomes $\frac{1}{3}\mathrm{Tr}(\boldsymbol{\alpha}_2)/\bar{\alpha}_2$, i.e. (arithmetic mean of principal components)/(geometric mean of principal components).

The correction is modest, except for strongly elongated ellipsoids. In SnTe, we estimate from the band structure calculations of Melvin and Hendry (1979) that the best principal values of $\boldsymbol{\alpha}$ to take at energies near the Fermi energy of the systems S1 and S2 are α_l (along the Σ axis) = 4.0, $\alpha_{t\Sigma}$ (transverse to the Σ axis, and in a (001) plane containing 4 Σ axes) = 6.7, $\alpha_{t\perp}$ (transverse to the Σ axis, and normal to the Σ plane) = 0.5. These values give

$$v(\hat{\boldsymbol{n}}) = 1.25\,\bar{v} \qquad \text{(independent of } \hat{\boldsymbol{n}}\text{)}.$$

For GaSb, the conclusion '$v(\hat{\boldsymbol{n}})$ independent of $\hat{\boldsymbol{n}}$' also applies because of the cubic symmetry, but we do not have data on the eccentricity of the L pockets.

In Bi, $\nu_2 = 1$, and the principal inverse masses of the holes are (Smith *et al* 1964) $\beta_3 = 1.45$ (along the trigonal axis) and $\beta_1 = \beta_2 = 15.6$ (normal to the trigonal axis). Then $v(\hat{\boldsymbol{n}})/\bar{v}$ varies between a minimum of 0.45 for the trigonal direction and a maximum of 1.5 for directions in the basal plane.

In the ellipsoidal model, the condition for absence of Landau damping by pocket μ of component 2 is

$$v(\hat{\boldsymbol{n}}) > |\boldsymbol{v}_{F_{2\mu}} \cdot \hat{\boldsymbol{n}}|_{\max}.$$

Calculation of the right side of this inequality leads to

$$v(\hat{\boldsymbol{n}}) > \bar{v}_{F_2} (\hat{\boldsymbol{n}} \boldsymbol{\alpha}_{2\mu} \hat{\boldsymbol{n}} / \bar{\alpha}_2)^{1/2} \tag{A1.2}$$

where $\bar{v}_{F_2}$ is the Fermi velocity of component 2 in the equivalent spherical model. We have applied this result to SnTe and Bi. For SnTe, with $\hat{n} \sim [001]$, there is weak Landau damping by a symmetry set comprising 8 of the 12 Σ pockets. For $\hat{\boldsymbol{n}} \sim [110]$, there is Landau damping by 2 of the 12 pockets. We think it likely that in these cases an acoustic plasmon will exist. For $\hat{\boldsymbol{n}} \sim [111]$, all 12 pockets contribute Landau damping, and we do not expect an acoustic plasmon.

For Bi, the $\boldsymbol{n}$ dependence is the same in equation (A1.2) as in equation (A1.1), because $\nu_2 = 1$. Consequently the conclusion of the spherical model applies: an acoustic plasmon exists for all $\hat{\boldsymbol{n}}$, but only just. q_c will be small in every direction.

References

Ashkenazi J, Kuper C G and Tyk R 1987 *Physics* **148** B 366–70
Bennacer B and Cottey A A 1989 *J. Phys.: Condens. Matter* **1** 1809–29
Canright G S and Vignale G 1988 *Phys. Rev. Abstracts* **19** 39
Cohen M L and Tsang Y W 1971 *The Physics of Semimetals and Narrow Gap Semiconductors* ed Carter D L and Bate R T (New York: Pergamon) pp 303–17
Cottey A A 1985 *J. Phys. F: Met. Phys.* **15** L203–6
Cottey A A, Enders R, Finkenrath H, Stoeckel T and Uhle N 1987 *Thin Solid Films* **149** 149–61
Farr M K, Traylor J G and Sinha S K 1975 *Phys. Rev.* B **11** 1587–94
Fistul' V I 1969 *Heavily Doped Semiconductors* (New York: Plenum) p 32
Gerlach E, Grosse P, Rautenberg M and Senske W 1976 *Phys. Status Solidi* b **75** 553–8
Griffin A 1988 *Phys. Rev.* B **37** 5943–6
Hilsum C 1966 *Semiconductors and Semimetals* (ed R K Willardson and A C Beer) vol 1 p 9
Hilsum C and Rose-Innes A C 1961 *Semiconducting III–V Compounds* (Oxford: Pergamon)
Jantsch W, Bussmann-Holder A, Bilz H and Vogl P 1983 *The Dynamical Properties of IV-VI Compounds* (Berlin: Springer)
Kauschke W, Mestres N and Cardona M 1987 *Phys. Rev.* B **36** 7469–85
Little W A 1988 *Science* **242** 1390–5
McWhorter A L and May W G 1984 *IBM J. Res. Dev.* **8** 285–90
Melvin J S and Hendry D C 1979 *J. Phys. C: Solid State Phys.* **12** 3003–12
Olivei A 1971 *Optik* **34** 153–70
Pinczuk A, Shah J and Wolff P A 1981 *Phys. Rev. Lett.* **47** 1487–90
Riedl H R, Dixon J R and Schoolar R B 1965 *Solid State Commun.* **3** 323–5
Ruvalds J 1981 *Adv. Phys.* **30** 677–95
—— 1987 *Phys. Rev.* B **35** 8869–72
Silin V P 1952 *Zh. Eksp. Teor. Fiz.* **23** 649–59
Smith G E, Baraff G A and Rowell J M 1964 *Phys. Rev.* **135** A1118–24
Vigneron J P, Lambin P, Lucas A A and Morawitz H 1988 *Physica* C **153–5** 1313–4